Interplay of Axial Ligation, Hydrogen Bonding, Self-Assembly, and Conformational Landscapes in High-Spin Ni(II) Porphyrins

ARTICLE *in* THE JOURNAL OF PHYSICAL CHEMISTRY B · JANUARY 2004

Impact Factor: 3.3 · DOI: 10.1021/jp036398d

4 AUTHORS, INCLUDING:

Mark Renner

72 PUBLICATIONS **2,515** CITATIONS

SEE PROFILE

Mathias O. Senge

Trinity College Dublin

375 PUBLICATIONS **5,836** CITATIONS

SEE PROFILE

Interplay of Axial Ligation, Hydrogen Bonding, Self-Assembly, and Conformational Landscapes in High-Spin Ni(II) Porphyrins

Kathleen M. Barkigia,[†] Mark W. Renner,[†] Mathias O. Senge,[‡] and Jack Fajer*[,†]

Materials Science Department, Brookhaven National Laboratory, Upton, New York 11973-5000, and Institute of Chemistry, Potsdam University, D-14476 Golm, Germany

Received: August 12, 2003; In Final Form: November 25, 2003

The molecular structures of four bis-ligated high-spin Ni(II) complexes of the sterically crowded, nonplanar 2,3,7,8,12,13,17,18-octaethyl-5,10,15,20-tetranitroporphyrin (NiOETNP) are reported. The ligands are imidazole (Im), imidazole plus 2-methylimidazole (2-MeIm) in the crystal lattice, 1-methylimidazole (1-MeIm), and 2,1,3-benzoselenadiazole (BSeD). Extensive intermolecular hydrogen bonding is observed in the three imidazole-ligated structures consisting of NH···O and CH···O bonding from the imidazoles to neighboring nitro groups and of NH···N interactions to a nearby 2-MeIm. The different modes of hydrogen bonding, typical of those frequently observed in proteins, mediate the self-assembly of discrete porphyrin dimers as well as more extensive two- and three-dimensional arrays. Only the bis-BSeD complex remains monomeric. The presence or absence of the different types of hydrogen bonds controls the orientations of the axial ligands and also modulates the conformations of the porphyrin skeletons. This interplay of axial ligation, hydrogen bonding, and self-assembly further illustrates the multiconformational landscapes that porphyrins can access as a function of their microenvironment. Such nonplanar deformations have been shown to significantly affect the optical, redox, magnetic, radical, and excited state properties of porphyrin derivatives. That hydrogen bonding can influence ligand interactions with neighboring functional groups as well as macrocycle conformations with their concomitant consequences on physical and chemical properties may thus be particularly relevant to the bioenergetic roles of porphyrin in vivo. These results also raise the question whether point mutations near porphyrins in vivo are structurally, and consequently functionally, innocent.

Introduction

The improving crystallographic resolution of photosynthetic reaction centers[1] and antennae[2] as well as of heme proteins[3] is increasingly revealing that the porphyrin macrocycles within the protein complexes are quite flexible and can adopt multiple nonplanar conformations. Theoretical calculations based on the crystallographic data for the photosynthetic chromophores suggest that these deviations from planarity affect both the redox and optical properties of the molecules.[4] The axial ligands, ubiquitous hydrogen bonds, and nearby residues that constitute the microenvironments of the photosynthetic chromophores and heme prosthetic groups must thus define the protein scaffolds that control the conformations of the macrocycles and thereby further fine-tune the inherent physical and chemical properties of the porphyrins.

An expanding body of structural data of isolated porphyrins, chlorins, bacteriochlorins, and isobacteriochlorins further illustrates the considerable plasticity of such molecules and the significant distortions that porphyrinic macrocycles can adopt.[3,5] In particular, multiple peripheral substituents, which impose steric constraints and thus act as primitive protein scaffolds, induce significant and multiple deformations. In turn, these distortions have been shown to modulate the optical, redox, magnetic, radical, and excited state properties of the chromophores[4,5] and thus begin to document and model the consequences of the distortions observed in proteins.

Photosynthetic reaction centers,[6] light-harvesting antenna complexes,[7] and heme proteins[8] have recently been reconstituted with nickel chlorophylls, bacteriochlorophylls, and porphyrins which serve both as spectroscopic probes and to modulate redox potentials and electron or energy transfer. Current interest in the chemistry of carbon dioxide has also focused attention on F430, the sole bacterial tetrapyrrole to contain nickel. The cofactor mediates the final states of the conversion of CO_2 to hydrocarbons in methanogenic bacteria.[9] Here again, hydrogen bonding and the protein environment are postulated to determine the conformation of the cofactor in vivo.[9,10]

Nonplanar Ni porphyrins exhibit significantly altered physical and chemical properties in comparison to planar Ni porphyrins. In addition to redox and optical shifts,[11] the distortion has been shown to affect sites of oxidation (Ni(III) vs Ni(II) π-cation radicals),[12,13] mixing of the two highest occupied orbitals in cation radicals,[14] spin states and orbital occupancy (d_{z^2} vs $d_{x^2-y^2}$ in Ni(III)),[12,13] and to induce dramatic changes in (d, d) excited state lifetimes[15] as well as influence ligation and deligation photophysics.[16] Many of these properties are attributed to the ability of the nonplanar Ni complexes to adopt or traverse multiple conformational landscapes.[12,13,15] Indeed, crystallography has provided ample evidence of such flexibility and polymorphism,[5,16−18] most recently illustrated by the different conformations induced by a single nearby aromatic group.[19]

We extend these structural studies here to the ligated, high-spin Ni(II) complexes of the nonplanar 2,3,7,8,12,13,17,18-octaethyl-5,10,15,20-tetranitroporphyrin (NiOETNP).[18] The interplay between hydrogen bonding, axial ligation, nearby

* Author to whom correspondence should be addressed. E-mail: fajerj@bnl.gov. Fax: (631) 344-5815.
[†] Brookhaven National Laboratory.
[‡] Potsdam University.

10.1021/jp036398d CCC: $27.50
Published on Web 01/29/2004

TABLE 1: Crystallographic Data

	1	**2**	**3**	**4**
chemical formula	$NiN_8C_{36}H_{40}O_8 \cdot 2(C_3H_4N_2) \cdot C_4H_6N_2)$	$NiN_8C_{36}H_{40}O_8 \cdot 2(C_4H_6N_2) \cdot C_4H_6N_2)$	$NiN_8C_{36}H_{40}O_8 \cdot 2(C_3H_4N_2) \cdot CH_2Cl_2)$	$NiN_8C_{36}H_{40}O_8 \cdot 2(SeC_6H_4N_2) \cdot SeC_6H_4N_2)$
fw (g/mol)	989.74	1017.79	992.56	1320.69
space group	$P\bar{1}$	$P2_1/n$	$P\bar{1}$	$P2_1/c$
T, K	145	100	107	293
a, Å	13.181(2)	14.351(2)	12.795(2)	18.917(2)
b, Å	13.563(1)	22.677(2)	13.686(2)	23.658(2)
c, Å	14.545(2)	15.373(2)	15.496(2)	12.853(1)
α, °	91.87(1)	90.00	107.75(1)	90.00
β, °	96.19(1)	103.05(1)	104.22(1)	105.10(1)
γ, °	110.94(1)	90.00	106.73(2)	90.00
V, Å^3	2407.3(5)	4873.7(10)	2303.7(6)	5553.6(9)
Z	2	4	2	4
λ, Å	0.9398	0.9100	0.9391	1.54178
D_c, g/cm^3	1.365	1.387	1.431	1.580
μ, mm^{-1}	0.471	0.467	0.603	3.313
R1 ($F_o > 4\sigma(F_o)$)	0.050	0.058	0.072	0.102
wR2 (all data)	0.132	0.157	0.200	0.329

"residues", and the different conformational landscapes observed further illustrates the plasticity of the macrocycles as well as their acute structural sensitivity to their microenvironment, effects increasingly seen both in vitro and in vivo. These evidently facile interconversions and multiplicities of conformational surfaces ("surfing") also raise the caveat that site-directed mutations in proteins may not be structurally innocent by affecting the conformations and hence the properties of the porphyrinic prosthetic groups and chromophores. Such conformational effects may influence electron transfer in bacterial photosynthetic reaction centers. Indeed, mutations at or near the chromophores that carry out the primary photochemical charge separation have been shown to affect the energetics and dynamics of charge transfer,[20] even to the point of redirecting electron flow along the normally nonfunctional B branch of wild-type reaction centers.[21] As well, Laible et al.[22] have recently noted that both natural variations in wild-type photosynthetic bacteria and site-specific mutations near the cofactors modulate triplet energy transfer rates from the primary donors to carotenoids. This critical photoprotective mechanism is a short range Dexter[23] process that requires near orbital overlap between donor and acceptor and is thus particularly sensitive to small structural changes induced by variations in the environment of the chromophores[24] as clearly illustrated here by the multiple conformations adopted by the in vitro models as a function of hydrogen bonding and axial ligation.

Experimental Methods

NiOETNP was synthesized as previously described.[18] Imidazole (Im), 1-methylimidazole (1-MeIm), 2-methylimidazole (2-MeIm), and 2,1,3-benzoselenadiazole (BSeD) were purchased from Aldrich and used without further purification. Optical spectra in CH_2Cl_2 were recorded on a Cary 500 spectrophotometer for solutions prepared with ~10:1 ratios of ligand to porphyrin. (Even much larger ratios of BSeD to porphyrin offered no spectral evidence of ligation by BSeD in CH_2Cl_2.)

Crystals of the ligated complexes, including those of $(BSeD)_2$, were obtained by diffusion of pentane into CH_2Cl_2 solutions. The complex labeled $(Im)_2$ + 2-MeIm was obtained from solutions that adventitiously contained ~10% 2-MeIm in addition to Im.

Select crystallographic experimental data are presented in Table 1 and additional details are included in the Supporting Information. Data for all the imidazole-ligated species (**1**−**3**) were collected at beamlines X7B or X12C of the National Synchrotron Light Source at Brookhaven, whereas data for the BSeD complex (**4**) were measured on an Enraf-Nonius CAD4 diffractometer equipped with a Cu tube. For **1**−**3**, at least one hemisphere of data was collected by the rotation method on an area detector and processed with Denzo/Scalepack. The serial data for **4** were measured in $\theta/2\theta$ mode and reduced using XCAD4VAX. Lattice parameters for the synchrotron data were determined separately for each recorded image and are mean values derived from the reproducibility of the determinations. Those for the CAD4 data were based on 25 high-angle reflections. The structures were solved by direct methods and refined against F^2 using SHELXL-93 in the SHELXTL version 5 package. Hydrogens were included in idealized positions using a riding model. Coordinates, bond distances, and angles are available in CIF format in the Supporting Information.

Results and Discussion

The structural consequences of forming the bis-ligated high-spin Ni(II) OETNP were investigated using four different axial ligands: 2,1,3-benzoselenadiazole (BSeD), **4**, a potential bidentate ligand;[13] imidazole (Im), **3**; 1-methylimidazole (1-MeIm), **2**; imidazole plus 2-methylimidazole (2-MeIm), **1**. The optical changes caused by conversion of the low-spin NiOETNP to high-spin Ni(II) in CH_2Cl_2 are shown in Figure 1. (Even high concentrations of BSeD do not induce any optical changes in CH_2Cl_2. Nonetheless, crystals of the $(BSeD)_2$−Ni complex were obtained suggesting that ligation occurs only at concentration profiles that favor crystallization.) In addition to the red-shifts of the visible and Soret bands typically observed on conversion of low- to high-spin Ni(II) porphyrins,[16,24] the Soret bands of the ligated NiOETNPs split. The high-energy component of the Soret band has been attributed[24] to a porphyrin-to-nitro group charge-transfer band in the case of the bis-pyridine complex which exhibits an optical spectrum comparable to those reported here (Figure 1). The similarity of the spectra with the different axial ligands thus suggests common configurations for all the ligated species in solution.

In contrast to the results in solution, the crystal structures of the four complexes with different axial ligands reveal extensive differences in the conformations of the porphyrins and orientations of the axial ligands as well as extensive and different types of hydrogen bonding which, in turn, promote different modes of aggregation of the porphyrins.

The molecular structures of the four bis-ligated complexes are shown in Figures 2 and 3, and a detailed comparison of the

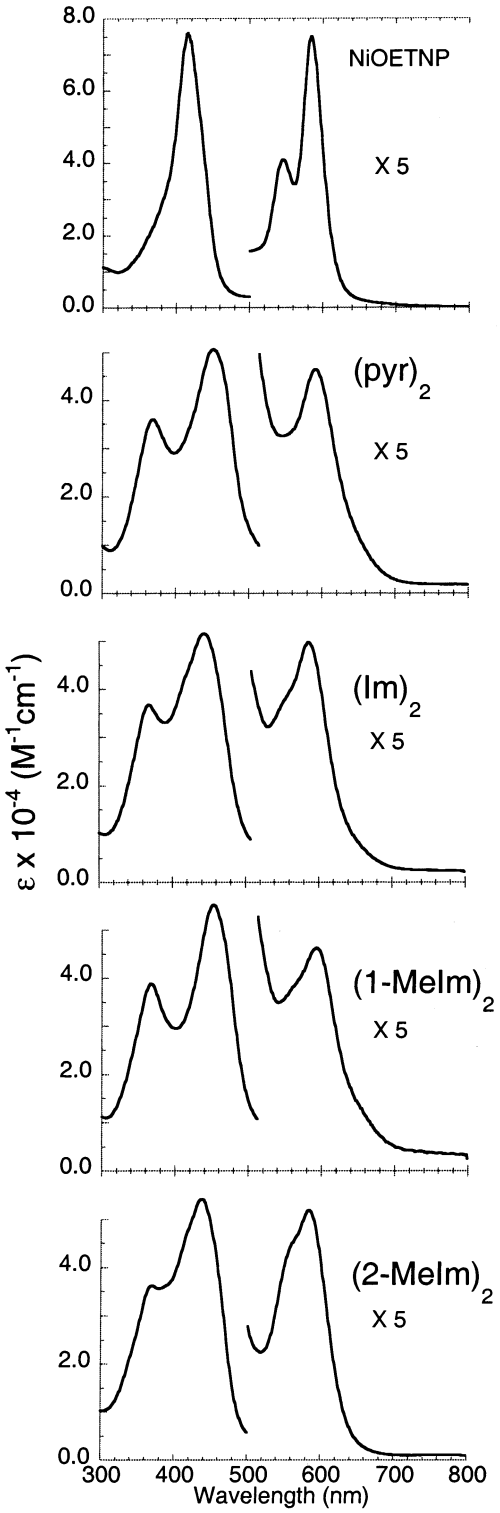

Figure 1. Optical spectra in CH_2Cl_2 of the unligated, low-spin Ni(II) OETNP and of the ligated, high-spin complexes with the ligands shown.

metrics for the four complexes is presented in Table 2. In each structure, the crystallographic asymmetric unit consists of a complete porphyrin with two axial ligands bound to the Ni via nitrogens and a molecule of crystallization which is 2-MeIm in **1**, 1-MeIm in **2**, CH_2Cl_2 in **3**, and BSeD in **4**. Except in **1**, the solvates are "innocent", occupy voids in the lattice, and are well-separated from the porphyrin.

In all four complexes, the Ni(II) is high spin with $(d_{x^2-y^2})^1$ and $(d_{z^2})^1$ orbital occupancies as evidenced by both the long equatorial and axial Ni−N distances. The average equatorial Ni−N distances to the porphyrin expand from 1.920(4) Å in the low-spin unligated compound[18] to 2.067(5), 2.051(2), 2.051(8), and 2.045(7) Å in **1**, **2**, **3**, and **4**, respectively, values typical of high-spin Ni(II) porphyrins[12,13,16,18,25,26] and indicative of the repulsive effects of the electron in the Ni $d_{x^2-y^2}$ orbital on the porphyrin nitrogens. The Ni−N distances to the axial ligands also reflect the high-spin Ni configuration with the second unpaired electron in the d_{z^2} orbital. These distances are essentially equivalent to the 1-MeIms in **2**, 2.155(3) and 2.160(3) Å, and to the Ims in **3**, 2.168(8) and 2.158(8) Å, values comparable to those of 2.160−2.174 Å reported for other imidazole-ligated Ni(II) porphyrins.[26] In **1**, the axial distances differ by $\sim 5\sigma$, 2.159(6) Å to N1A and 2.134(5) Å to N2A, and likely result from the different strengths and types of hydrogen bonds (NH···N and NH···O) of the exterior nitrogens of the imidazoles (vide infra). The Ni−N bonds to the BSeDs in **4** are significantly longer, reflecting both steric constraints of the bulkier ligand and the fact that BSeD is a significantly poorer base than the imidazoles. (Recall that BSeD does not bind to the porphyrin in CH_2Cl_2 solution.) In addition, one of the ligating BSeDs, comprised of N2A, Se2, and so forth, adopts two distinct configurations relative to the equatorial N−Ni−N axis resulting in three different and long axial Ni−N distances of 2.227(7) Å to N1A, 2.240(15) Å to N2A, and 2.278(15) Å to N2B. (Atomic nomenclature for the second orientation of the disordered BSeD, N2B, Se2B, etc., not shown in Figure 3, is included in the Supporting Information.) An analogous high-spin Ni(II) complex, the cation radical of octaethyltetraphenylporphyrin with 2,1,3-benzothiadiazole ligands, has been structurally characterized[13] and exhibits comparable Ni−N axial distances of 2.23(2) Å.

Hydrogen bonds have long been recognized as important intermolecular interactions that play a significant role in determining molecular conformation, molecular aggregation, and the functions of inorganic as well as biological systems.[27] Salient features of the three imidazole complexes reported here are the variety of hydrogen-bonding modes between the axial ligands and nitro groups of adjacent porphyrins which lead to different types of self-assembly and conformations of the porphyrins, see Figures 4−7.

In **2**, the molecules pack as dimers (Figure 5) linked by reciprocal CH···O hydrogen bonds from a C−H of one of the axial 1-MeIms (C5A) to the oxygen of a nitro group (O1) of an adjacent molecule with a carbon-to-oxygen distance of 3.05 Å, a value well within those attributed to CH···O bonds in nucleic acids, proteins, and a variety of organic compounds.[27,28] Interestingly, as in the present case, Derewanda et al.[29] have noted that it is the C−H fragments located between the two nitrogens of histidine imidazoles that form hydrogen bonds to oxygens in serine hydrolases. In **2**, the hydrogen-bonded 1-MeIm subtends a wider dihedral angle ϕ[30] of 19° relative to the equatorial N−Ni−N axis than the unbound ligand which forms an angle of 6°. The peripheral hydrogen bond has thus rotated the axial ligand to facilitate the dimer formation. The two ligands sit at 67° to each other. (A value of 0° means that the planes of the two axial ligands are parallel, whereas an angle of 90° means that they are orthogonal.)

Unlike **2**, in which the exterior nitrogen of the 1-MeIm is blocked, the imidazoles of **3** and **1** do form hydrogen bonds at that position. In **3**, both Ims participate in hydrogen bonds which result in infinite chains that are cross-linked to a second set of chains (Figure 6). One Im forms a bifurcated hydrogen bond to a nitro group within a chain with a major NH···O component[27] at a nitrogen-to-oxygen distance of 2.98 Å and a second, minor component[27] NH···O bond at a nitrogen-to-oxygen distance of

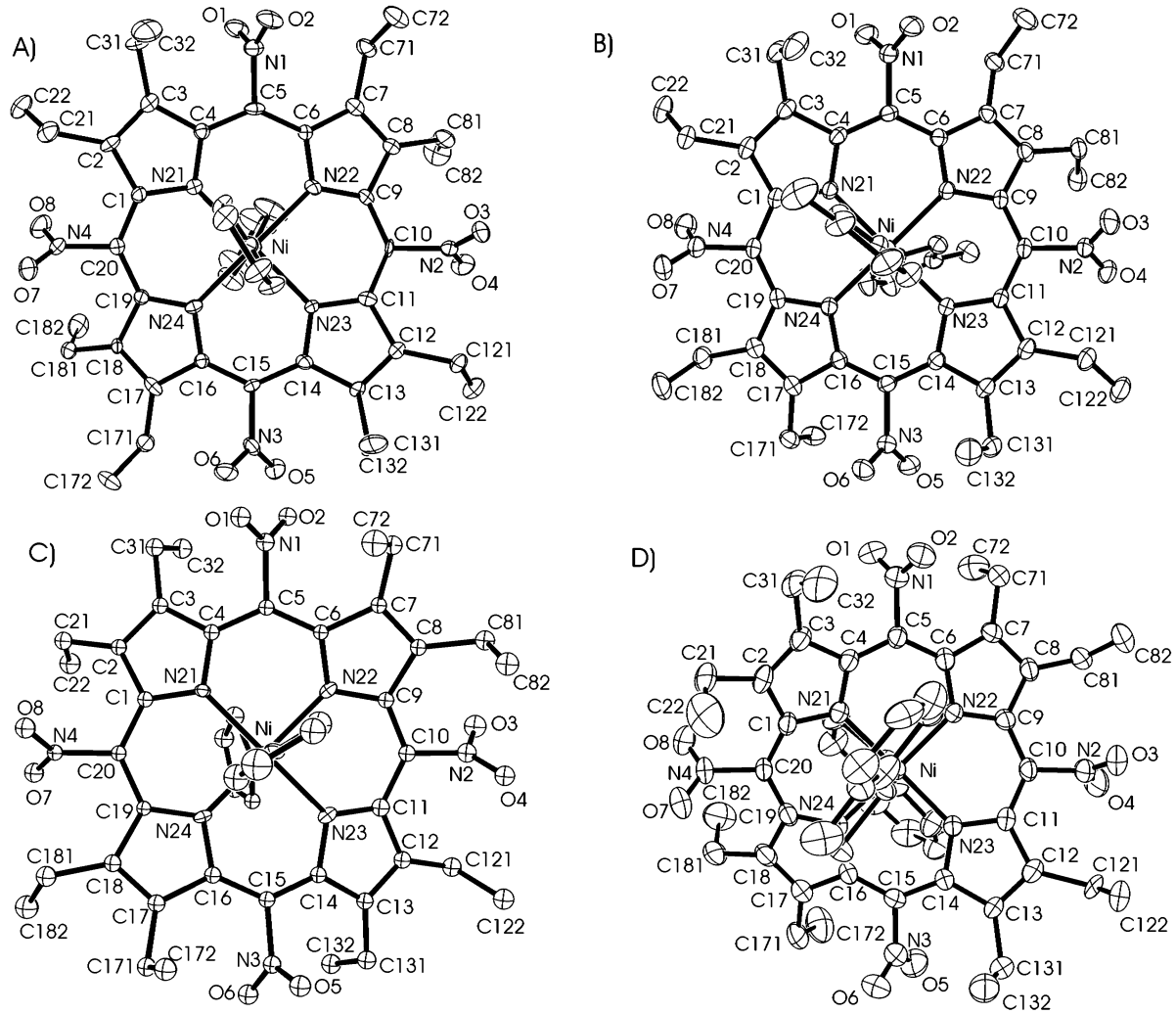

Figure 2. Molecular structures and atom names for the ligated NiOETNP(L)$_2$ complexes viewed from above: (a) (Im)$_2$ + 2-MeIm (not shown); (b) (1-MeIm)$_2$; (c) (Im)$_2$; (d) (BSeD)$_2$. Thermal ellipsoids enclose 30% probabilities. Hydrogens are omitted for clarity.

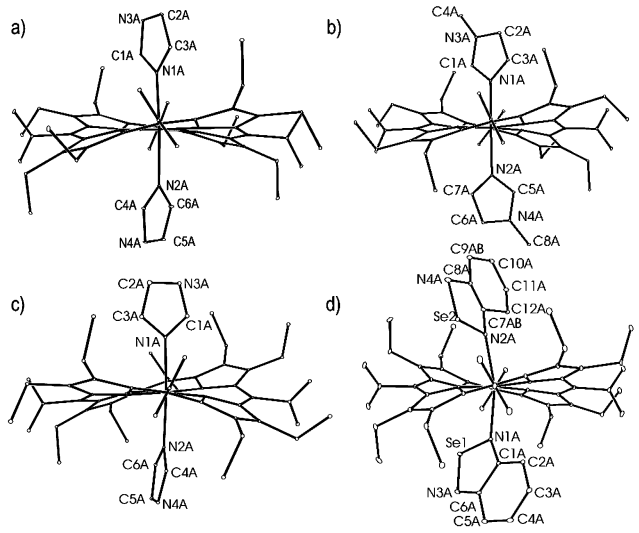

Figure 3. Edge-on views of the complexes and atom names for the ligands: (a) (Im)$_2$ + 2-MeIm (not shown); (b) (1-MeIm)$_2$; (c) (Im)$_2$; (d) (BSeD)$_2$.

3.14 Å. The second axial Im forms a single NH···O bond within a chain with a nitrogen-to-oxygen distance of 3.14 Å. The cross linkage of the Im with the bifurcated hydrogen bond causes the ligand to rotate significantly relative to the porphyrin N−Ni−N axis with $\phi = 35°$, whereas the second ligand which only forms hydrogen bonds within a chain is rotated less with $\phi = 13°$. Particularly noteworthy are the effects observed in **1** which incorporates a 2-MeIm in the crystal lattice in addition to the two imidazole axial ligands and results in a strikingly different hydrogen-bonded assembly. As shown in Figure 7, the porphyrins in **1** are the building blocks of an infinite polymeric network which also includes the 2-MeIm of crystallization. Each imidazole does participate in a hydrogen bond. At one end, the exterior nitrogen of the Im is a donor to the unprotonated nitrogen of the 2-MeIm forming an NH···N bond with a nitrogen-to-nitrogen distance of 2.85 Å and resulting in the Im being rotated to $\phi = 13°$. In turn, the N−H of the 2-MeIm is a donor to a nitro group of an adjacent porphyrin forming an NH···O bond with a nitrogen-to-oxygen distance of 2.95 Å. At the other end, the external nitrogen of the second axial Im acts as a donor to another porphyrin nitro group forming an NH···O bond with a nitrogen-to-oxygen distance of 3.03 Å with the Im rotated to $\phi = 16°$. (The very different environments at the periphery of the axial ligands may also contribute to the variations of the axial Ni−N distances, 2.159(6) Å vs 2.134(5) Å noted above.) The inclusion of the 2-MeIm in the hydrogen-bonded assembly of **1** is remarkable given that the 2-MeIm was only present in ∼10% of the concentration of the Ims in the crystallization medium. The resulting network with the ad-

TABLE 2: Summary of Displacements (Å), Distances (Å), and Angles (deg) in NiOETNPs

	NiOETNP $(Im)_2(2MeIm)$ **1**	NiOETNP $(1MeIm)_2$ **2**	NiOETNP $(Im)_2$ **3**	NiOETNP $(BSeD)_2$ **4**
Ni[a]	0.03	0.04	0.02	0.02
N[a]	0.04	0.05	0.05	0.09
Cm[a]	0.17	0.06	0.25	0.03
Cα[a]	0.22	0.28	0.27	0.32
Cβ[a]	0.63	0.78	0.76	0.84
Δ24 atoms	0.32	0.37	0.39	0.41
angle of ligand vs porphyrin mean plane, deg	86, 84	87, 80	89, 78	68 71, 70
ϕ (vs N−Ni−N axis), deg	13, 16	6, 19	13, 35	18 17, 13
relative dihedral angle of ligands, deg	63	67	69	88 89
dihedral angle of NO_2, deg	68, 69, 57, 61 63.8 (av)	54, 58, 64, 59 58.8 (av)	55, 56, 62, 63 59.0 (av)	58, 65, 60, 53 59.0 (av)
Ni−N (axial), Å	2.159(6) 2.134(5)	2.155(3) 2.160(3)	2.168(8) 2.158(8)	2.227(7) 2.240(15) 2.278(15)
Ni−N (porphyrin), Å	2.067(5)	2.051(2)	2.051(8)	2.045(7)
Ct−N	2.067(5)	2.051(2)	2.051(8)	2.045(7)
Ct−Cm	3.372	3.355	3.363	3.355
N−Cα	1.367(7)	1.360(4)	1.372(12)	1.365(11)
Cα−Cβ	1.466(8)	1.458(4)	1.465(14)	1.462(13)
Cα−Cm	1.401(9)	1.394(4)	1.402(13)	1.395(13)
Cβ−Cβ	1.360(8)	1.355(4)	1.356(13)	1.350(14)
Cm−NO_2	1.482(8)	1.475(4)	1.475(13)	1.489(12)
N−Ni−N (opp), deg	177.2(2)	176.9(2)	177.1(3)	175.2(3)
N−Ni−N (adj)	90.0(2)	90.0(4)	90.1(3)	90.1(3)
Ni−N−Cα	126.0(4)	125.4(4)	125.8(6)	125.3(5)
N−Cα−Cm	121.0(6)	120.9(3)	120.4(9)	120.6(8)
N−Cα−Cβ	110.4(5)	110.3(2)	111.7(8)	110.1(8)
Cα−N−Cα	106.3(5)	106.4(2)	105.9(8)	106.4(7)
Cα−Cm−Cα	131.6(6)	130.6(3)	130.8(9)	130.3(8)
Cα−Cβ−Cβ	106.4(5)	106.4(3)	106.5(8)	106.6(8)
Cm−Cα−Cβ	128.6(5)	128.9(3)	129.2(9)	129.2(8)

[a] Displacements in Å from the mean plane of the 24 core atoms of the macrocycle.

ditional hydrogen bonds must therefore be thermodynamically favored. The structural differences between **1** and **3** may also provide a primitive protein model of the consequences of point mutations that introduce (or remove) residues capable of hydrogen bonding near chromophores or prosthetic groups in vivo. Only in **4**, in which the BSeDs do not hydrogen bond, does the porphyrin remain monomeric. As well, the absence of any hydrogen-bonding interactions likely accounts for the disorder of one of the BSeDs resulting in different axial Ni−N distances (and obviously ϕ orientations) of the disordered ligand (Table 2).

As noted above and shown in Figure 4, the porphyrins display different conformational landscapes which vary with the axial ligands, the types of hydrogen bonds, and the modes of self-assembly. These macrocyclic distortions are further illustrated in the histograms presented in Figure 8 which plot the average displacements of the meso and β-carbons and the average deviations of the 24 core atoms of the porphyrin from the least-squares plane defined by the 24 atoms. The nomenclature that describes the types of distortions commonly observed in nonplanar porphyrins was originally suggested by Scheidt and Lee.[30] In a saddle conformation, alternate pyrrole rings tilt up and down with respect to the least-squares plane through the 24 atoms of the porphyrin core and the meso carbon atoms lie in the least-squares plane. In a ruffled conformation, alternate pyrrole rings twist clockwise or counterclockwise about the metal−nitrogen bond and the meso carbon atoms move alternately above or below the least-squares plane through the 24 atom core. As is evident from Figures 4 and 8, the four complexes adopt saddle conformations with increasing levels of superimposed ruffled distortions. Thus, **4** exhibits a saddle conformation and the three imidazole-ligated complexes adopt increasingly larger ruffled distortions in the order **2** < **1** < **3** as clearly reflected by the rising displacements of the meso carbons shown in Figure 8. Not surprisingly, because of the sterically encumbering multiple substituents, all four porphyrin complexes are significantly distorted with the average displacements of the 24 core atoms (Δ24 in Table 2) ranging between 0.32 Å in **1** to 0.41 Å in **4** in the order **4** > **3** > **2** > **1**.

Shelnutt[3,31] has developed a normal-coordinate structural decomposition method (NSD) which simulates any porphyrin distortion by linear combinations of six normal deformations that include, in addition to saddled (sad) and ruffled (ruf) distortions, domed (dom), waved[32] (wav(x) and wav(y)) and propeller (pro) conformations as well as yielding total out-of-plane displacements (D^{oop}). The results of an NSD analysis of **1**−**4** are presented in Table 3 and parallel the trends of the histograms in Figure 8, that is, the total distortions (D^{oop}) increase in the order **1** < **2** < **3** < **4**, the saddling decreases in the order **4** > **2** > **3** > **1**, and the ruffling increases in the order **4** < **2** < **1** < **3**. The NSD calculations also assign sizable wave contributions to the distortions in **4**.

The above crystallographic results reveal several novel solid state features. Particularly noteworthy are the variety of hydrogen bonds between the different donor imidazole ligands and the acceptor nitro groups of the porphyrin, and those of the intercalated 2-MeIm in **1** which acts as both donor and acceptor. Cumulatively, these duplicate nearly the full panoply of hydrogen bonds found in proteins.[27,29] The multiple hydrogen bonds lead to several different modes of self-assembly that range

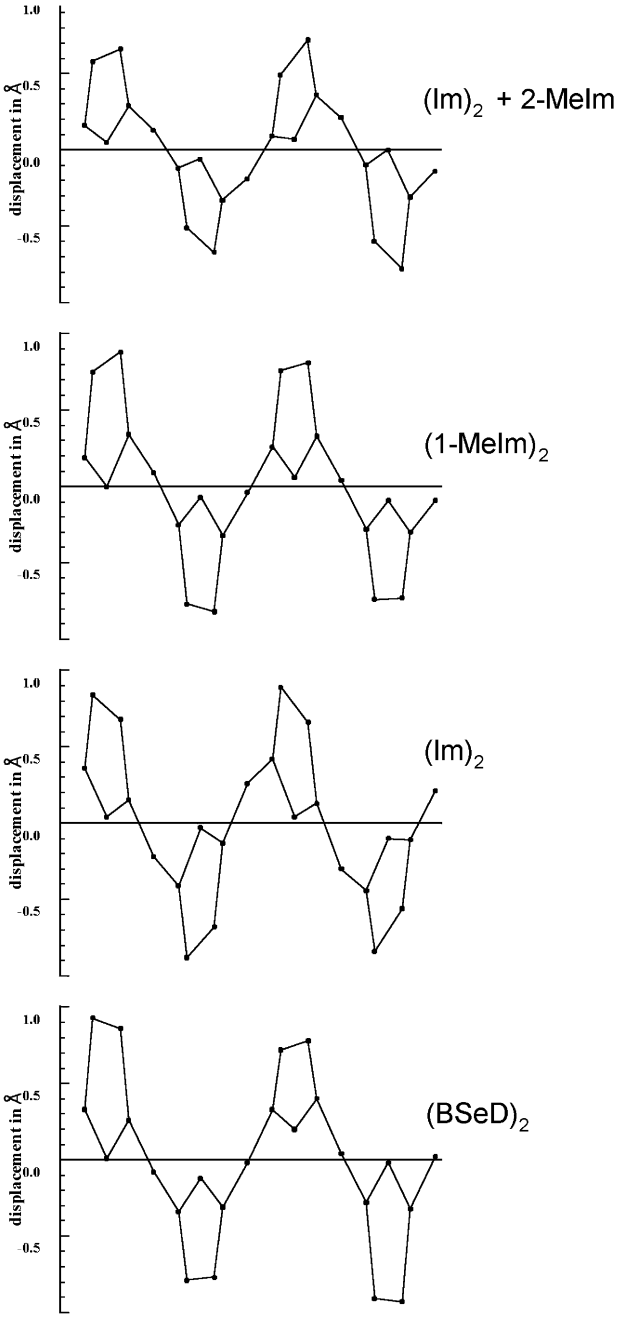

Figure 4. Linear displays of the out-of-plane displacements of the core atoms from the average plane of the 24 atoms for the four different ligated complexes. (The horizontal axis is not to scale.)

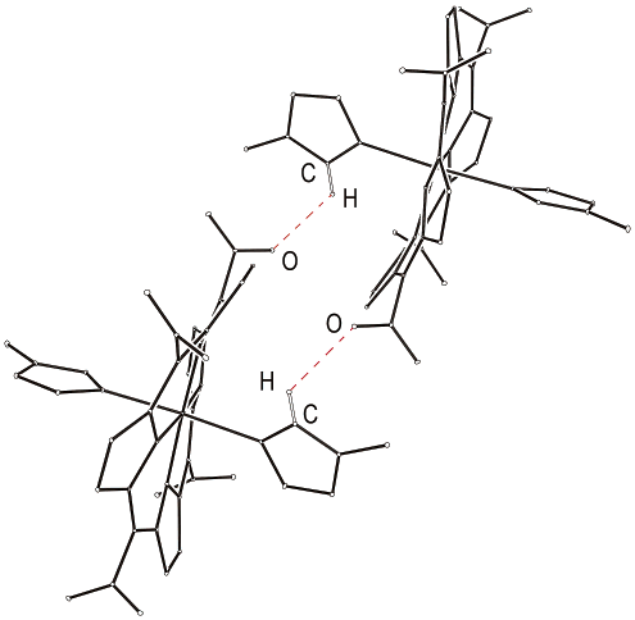

Figure 5. Dimer of the $(1\text{-MeIm})_2$ complex formed by C−H···O hydrogen bonds between a C−H of one 1-MeIm axial ligand and the oxygen of a nitro group on the adjacent porphyrin. The distances between the carbons and oxygens are 3.05 Å. Dihedral angles ϕ of the axial ligands relative to the N−Ni−N axis: 19° (bound) and 6° (unbound).

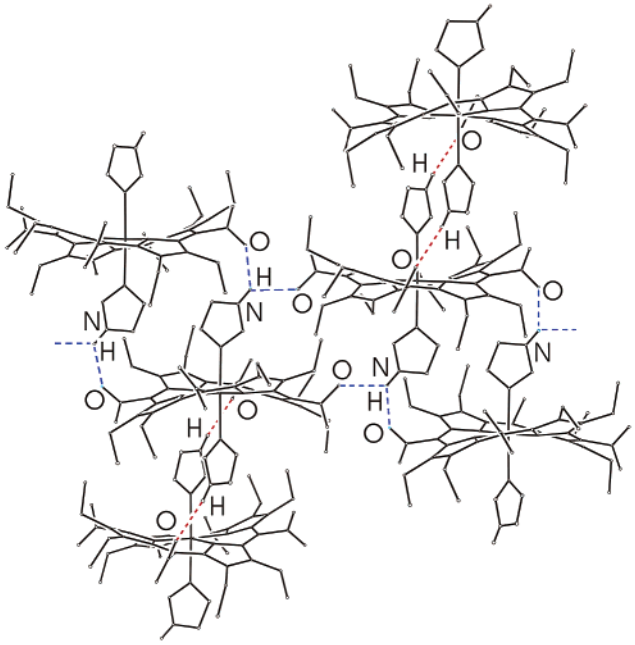

Figure 6. $(Im)_2$ complex. The imidazoles participate in two types of H-bonding. One axial ligand forms a bifurcated H-bond (shown in blue) to a nitro oxygen within a chain (N···O = 2.98 Å) *and* to a nitro group in the next chain (N···O = 3.14 Å). The second axial Im forms a single N−H···O bond (shown in red) within a chain (N···O = 3.14 Å). Dihedral angles ϕ: 35° (bifurcated H-bond) and 13° (single H-bond).

from dimer formation to two- and three-dimensional arrays and to multiple conformational landscapes. At the very minimum, these results further illustrate the plasticity of porphyrins in general and Ni porphyrins in particular. Normally, the conformation of the macrocycle controls the orientations of the axial ligands. In saddled distortions, the ligands align along the grooves formed by the saddle[13,16,33] and therefore eclipse the N−M−N axes ($\phi = 0°$) and orient perpendicular to each other (as in **4**), whereas in ruffled conformations the ligands tend toward staggered orientations[18,26,34] ($\phi = 45°$). It is clear from the present data that hydrogen bonding of the axial imidazoles enforces unexpected ligand orientations (as in **3** where $\phi = 13°$ *and* 35°) with much smaller relative orientations, 63° to 69°, than observed for the BSeD complex (88° to 89°) which is not hydrogen bonded. It is thus very likely that it is the combination of hydrogen-bonded self-assembly and ligand orientations that induces the multiplicity of conformations observed here.

Nonplanar distortions and particularly ruffled deformations in synthetic porphyrins have been shown to significantly alter the optical,[35] redox, magnetic, radical, and excited state properties of the molecules.[4,5,11,13−16,19,31,33−35] Such distortions, enforced by the protein scaffolding, thus provide an attractive and simple mechanism for fine-tuning the inherent physical and chemical properties of porphyrinic chromophores and prosthetic

TABLE 3: Normal Structural Decomposition (NSD) Calculations for NiOETNP(L)$_2$[a]

L	D_{obs}^{oop}	D_{sim}^{oop}	$\bar{\delta}_{oop}$	sad	ruf	dom	wav-*x*	wav-*y*	pro
1, Im + (2-MeIm)	1.950	1.935	0.0410	1.8610	0.5040	0.0480	0.1580	0.0270	0.0100
2, 1-MeIm	2.366	2.3490	0.0460	2.3370	0.1890	0.0660	0.0890	0.0200	0.0640
3, Im	2.381	2.3640	0.0470	2.2530	0.7010	0.0510	0.0350	0.1250	0.0470
4, BSeD	2.554	2.5410	0.0390	2.5250	0.0140	0.0570	0.1980	0.1870	0.0030

[a] Out-of-plane displacements (Å) using the minimal basis.

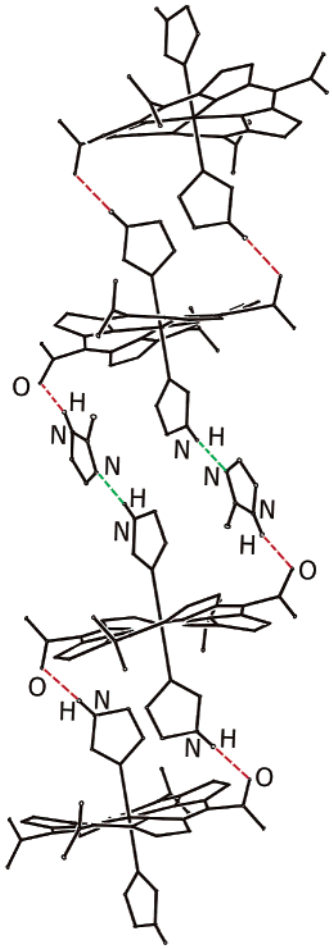

Figure 7. $(Im)_2$ complex + 2-MeIm. One Im (with $\phi = 13°$) is H-bonded to the nitro group of an adjacent porphyrin, N−H···O, with N···O = 3.03 Å. The second axial Im (with $\phi = 16°$) is H-bonded to the unprotonated nitrogen of the 2-MeIm in the lattice, N−H···N, with N···N = 2.85 Å. In turn, the NH of the 2-MeIm solvate is H-bonded to a nitro oxygen, N−H···O, with N···O = 2.95 Å.

groups in vivo[38] as well as a rationale for a functional role for the deformations of porphyrinic cofactors increasingly observed in protein crystal structures.[1−4] The present results illustrate the cumulative structural effects that hydrogen bonding can induce including significant variations in macrocycle conformations.[39] Taken as primitive protein models, these results suggest that point mutations in proteins which introduce or remove residues capable of hydrogen bonding may not be structurally, and hence functionally, innocent.

Acknowledgment. The work at Brookhaven National Laboratory was supported by the Division of Chemical Sciences, Geosciences and Biosciences, Office of Basic Energy Sciences, U.S. Department of Energy, under Contract DE-AC02-98CH10886. Financial support for the work at Potsdam University was provided by the Deutsche Forschungsgemeinschaft (Grant Se543/6-1).

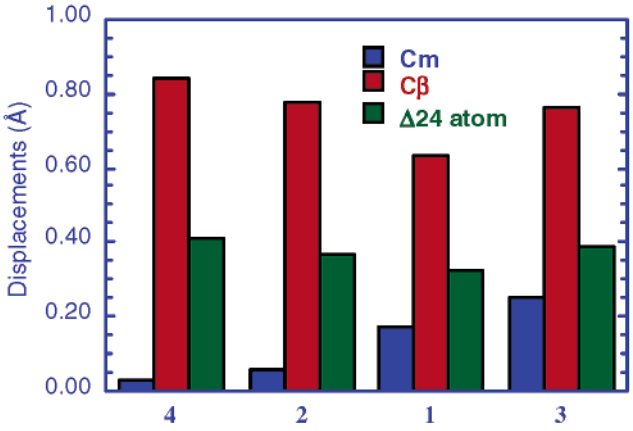

Figure 8. Histogram which compares the average out-of-plane displacements of the meso carbons, β-carbons, and average deviations from the 24-atom plane. Note the increasing degree of ruffling evidenced by the increasing displacements of the meso carbons.

Supporting Information Available: Crystallographic information files (in CIF format) for compounds **1**−**4**. This material is available free of charge via the Internet at http://pubs.acs.org.

References and Notes

(1) (a) Ermler, U.; Fritzsch, G.; Buchanan, S. K.; Michel, H. *Structure* **1994**, *2*, 925. (b) Deisenhofer, J.; Epp, O.; Sinning, I.; Michel, H. *J. Mol. Biol.* **1995**, *246*, 429. (c) Jordan, P.; Fromme, P.; Witt, H. T.; Saenger, W.; Krauss, N. *Nature* **2001**, *411*, 909. (d) Fyfe, P. K.; Jones, M. R. *Biochim. Biophys. Acta* **2000**, *1459*, 413.

(2) (a) Li, Y. F.; Zhou, W.; Blankenship, R. E.; Allen, J. P. *J. Mol. Biol.* **1997**, *271*, 456. (b) Prince, S. M.; Papiz, M. Z.; Freer, A. A.; McDermott, G.; Hawthornthwaite-Lawless, A. M.; Cogdell, R. J.; Isaacs, N. W. *J. Mol. Biol.* **1997**, *268*, 412. (c) McLuskey, K.; Prince, S. M.; Cogdell, R. J.; Isaacs, N. W. *Biochemistry* **2001**, *40*, 8738.

(3) Shelnutt, J. A. In *The Porphyrin Handbook*; Kadish, K. M., Smith, K. M., Guilard, R., Eds.; Academic Press: New York, 2000; Vol. 7, p 167.

(4) (a) Barkigia, K. M.; Chantranupong, L.; Smith, K. M.; Fajer, J. *J. Am. Chem. Soc.* **1988**, *110*, 7566. (b) Gudowska-Nowak, E.; Newton, M. D.; Fajer, J. *J. Phys. Chem.* **1990**, *94*, 5795.

(5) (a) Senge, M. O. In *The Porphyrin Handbook*; Kadish, K. M., Smith, K. M., Guilard, R., Eds.; Academic Press: New York, 2000; Vol. 1, p 239. (b) Fajer, J. *J. Porphyrins Phthalocyanines* **2000**, *4*, 382.

(6) (a) Chen, L. X.; Wang, Z.; Hartwich, G.; Katheder, I.; Scheer, H.; Scherz, A.; Montano, P. A.; Norris, J. R. *Chem. Phys. Lett.* **1995**, *234*, 437. (b) Hartwich, G.; Friese, M.; Scheer, H.; Ogrodnik, A.; Michel-Beyerle, M. E. *Chem. Phys.* **1995**, *197*, 423. (c) Zehetner, A.; Scheer, H.; Siffel, P.; Vacha, F. *Biochim. Biophys. Acta* **2002**, *1556*, 21.

(7) Fiedor, L.; Leupold, D.; Teuchner, K.; Voigt, B.; Hunter, C. N.; Scherz, A.; Scheer, H. *Biochemistry* **2001**, *40*, 3737.

(8) (a) Ma, J.-G.; Laberge, M.; Song, X.-Z.; Jentzen, W.; Jia, S.-L.; Zhang, J.; Vanderkooi, J. M.; Shelnutt, J. A. *Biochemistry* **1998**, *37*, 5118. (b) Venkateshrao, S.; Deepthi, S.; Pattabhi, V.; Manoharan, P. T. *Curr. Sci.* **2003**, *84*, 179.

(9) Ermler, U.; Grabarse, W.; Shima, S.; Goubeaud, M.; Thauer, R. K. *Science* **1997**, *278*, 1457.

(10) Todd, L. N.; Zimmer, M. *Inorg. Chem.* **2002**, *41*, 6831.

(11) (a) Barkigia, K. M.; Renner, M. W.; Furenlid, L. R.; Medforth, C. J.; Smith, K. M.; Fajer, J. *J. Am. Chem. Soc.* **1993**, *115*, 3627. (b) Senge, M. O.; Renner, M. W.; Kalisch, W. W.; Fajer, J. *J. Chem. Soc., Dalton Trans.* **2000**, 381. (c) Kadish, K. M.; Lin, M.; Van Caemelbecke, E.; De Stefano, G.; Medforth, C. J.; Nurco, D. J.; Nelson, N. Y.; Krattinger, B.; Muzzi, C. M.; Jaquinod, L.; Xu, Y.; Shyr, D. C.; Smith, K. M.; Shelnutt, J. A. *Inorg. Chem.* **2002**, *41*, 6673.

(12) Renner, M. W.; Fajer, J. *J. Biol. Inorg. Chem.* **2001**, *6*, 823; **2002**, *7*, 352.

(13) (a) Renner, M. W.; Barkigia, K. M.; Melamed, D.; Gisselbrecht, J.-P.; Nelson, N. Y.; Smith, K. M.; Fajer, J. *Res. Chem. Intermed.* **2002**, *28*, 741. (b) Renner, M. W.; Barkigia, K. M.; Melamed, D.; Smith, K. M.; Fajer, J. *Inorg. Chem.* **1996**, *35*, 5120.

(14) Lin, C.-Y.; Hu, S.; Rush, T.; Spiro, T. G. *J. Am. Chem. Soc.* **1996**, *118*, 9452.

(15) Drain, C. M.; Gentemann, S.; Roberts, J. A.; Nelson, N. Y.; Medforth, C. J.; Jia, S.; Simpson, M. C.; Smith, K. M.; Fajer, J.; Shelnutt, J. A.; Holten, D. *J. Am. Chem. Soc.* **1998**, *120*, 3781.

(16) Retsek, J. L.; Drain, C. M.; Kirmaier, C.; Nurco, D. J.; Medforth, C. J.; Smith, K. M.; Chirvony, V. S.; Fajer, J.; Holten, D. *J. Am. Chem. Soc.* **2003**, *125*, 9787.

(17) Barkigia, K. M.; Nurco, D. J.; Renner, M. W.; Melamed, D.; Smith, K. M.; Fajer, J. *J. Phys. Chem. B* **1998**, *102*, 322.

(18) (a) Senge, M. O. *J. Porphyrins Phthalocyanines* **1998**, *2*, 107. (b) Senge, M. O. *J. Chem. Soc., Dalton Trans.* **1993**, 3539.

(19) Nurco, D. J.; Smith, K. M.; Fajer, J. *Chem. Commun.* **2002**, 2982.

(20) (a) Lin, X.; Murchison, H. A.; Nagarajan, V.; Parson, W. W.; Allen, J. P.; Williams, J. C. *Proc. Natl. Acad. Sci. U.S.A.* **1994**, *91*, 10265. (b) Muh, F.; Williams, J. C.; Allen, J. P.; Lubitz, W. *Biochemistry* **1998**, *37*, 13066. (c) Katilius, E.; Katiliene, Z.; Lin, S.; Taguchi, A. K. W.; Woodbury, N. W. *J. Phys. Chem. B* **2002**, *106*, 12344.

(21) (a) Kirmaier, C.; He, C.; Holten, D. *Biochemistry* **2001**, *40*, 12132. (b) Kirmaier, C.; Laible, P. D.; Hanson, D. K.; Holten, D. *Biochemistry* **2003**, *42*, 2016. (c) Laible, P. D.; Kirmaier, C.; Udawatte, C. S. M.; Hofman, S. J.; Holten, D.; Hanson, D. K. *Biochemistry* **2003**, *42*, 1718.

(22) Laible, P. D.; Morris, Z. S.; Thurnauer, M. C.; Schiffer, M.; Hanson, D. K. *Photochem. Photobiol.* **2003**, *78*, 114.

(23) Dexter, D. L. *J. Chem. Phys.* **1953**, *21*, 836.

(24) Hobbs, J. D.; Majumder, S. A.; Luo, L.; Sickelsmith, G. A.; Quirke, J. M. E.; Medforth, C. J.; Smith, K. M.; Shelnutt, J. A. *J. Am. Chem. Soc.* **1994**, *116*, 3261.

(25) Ozette, K.; Leduc, P.; Palacio, M.; Bartoli, J.-F.; Barkigia, K. M.; Fajer, J.; Battioni, P.; Mansuy, D. *J. Am. Chem. Soc.* **1997**, *119*, 6442.

(26) (a) Duval, H.; Bulach, V.; Fischer, J.; Weiss, R. *Inorg. Chem.* **1999**, *38*, 5495. (b) Kirner, J. F.; Garofalo, J.; Scheidt, W. R. *Inorg. Nucl. Chem. Lett.* **1975**, *11*, 107.

(27) (a) Steiner, T. *Angew. Chem., Int. Ed.* **2002**, *41*, 48. (b) Jeffrey, G. A. *An Introduction to Hydrogen Bonding*; Oxford University Press: Oxford, 1997. (c) Jeffrey, G. A.; Saenger, W. *Hydrogen Bonding in Biological Structures*; Springer: Berlin, 1991.

(28) (a) Karle, I. L.; Ranganathan, D.; Haridas, V. *J. Am. Chem. Soc.* **1998**, *120*, 6903. (b) Song, J. S.; Szalda, D. J.; Bullock, R. M. *J. Am. Chem. Soc.* **1996**, *118*, 11134. (c) Steiner, T.; Saenger, W. *J. Am. Chem. Soc.* **1992**, *114*, 10146. (d) Taylor, R.; Kennard, O. *J. Am. Chem. Soc.* **1984**, *104*, 5063. (e) Wahl, M. C.; Sundaralingam, M. *Trends Biochem. Sci.* **1997**, *22*, 97. (f) Gu, Y.; Kar, T.; Scheiner, S. *J. Am. Chem. Soc.* **1999**, *121*, 9411.

(29) Derewenda, Z. S.; Derewenda, U.; Kobos, P. M. *J. Mol. Biol.* **1994**, *241*, 83.

(30) Scheidt, W. R.; Lee, Y. J. *Struct. Bonding* **1987**, *64*, 1.

(31) Sun, L.; Jentzen, W.; Shelnutt, J. A. The Normal Coordinate Structural Decomposition Engine. http://jasheln.unm.edu.

(32) Wave conformations were originally described more pictorially as "chairs" by Weiss and co-workers: Ochsenbein, P.; Ayouhou, K.; Mandon, D.; Fischer, J.; Weiss, R.; Austin, R. N.; Jayaraj, K.; Gold, A.; Terner, J.; Fajer, J. *Angew. Chem., Int. Ed. Engl.* **1994**, *33*, 348.

(33) (a) Renner, M. W.; Barkigia, K. M.; Fajer, J. *Inorg. Chim. Acta* **1997**, *263*, 181. (b) Ogura, H.; Yatsunyk, L.; Medforth, C. J.; Smith, K. M.; Barkigia, K. M.; Renner, M. W.; Melamed, D.; Walker, F. A. *J. Am. Chem. Soc.* **2001**, *123*, 6564. (c) Giraudeau, A.; Lobstein, S.; Ruhlmann, L.; Melamed, D.; Barkigia, K. M.; Fajer, J. *J. Porphyrins Phthalocyanines* **2001**, *5*, 763. (d) Medforth, C. J.; Muzzi, C. M.; Shea, K. M.; Smith, K. M.; Abraham, R. J.; Jia, S. L.; Shelnutt, J. A. *J. Chem. Soc., Perkin Trans. 2* **1997**, 833.

(34) (a) Barkigia, K. M.; Nelson, N. Y.; Renner, M. W.; Smith, K. M.; Fajer, J. *J. Phys. Chem. B* **1999**, *103*, 8643. (b) Jia, S.-L.; Jentzen, W.; Shang, M.; Song, X.-Z.; Ma, J.-G.; Scheidt, W. R.; Shelnutt, J. A. *Inorg. Chem.* **1998**, *37*, 7, 4402.

(35) Sterically crowded nonplanar porphyrins clearly exhibit large optical red-shifts compared to planar porphyrins. DiMagno, Ghosh and co-workers have argued that the red-shifts result from changes in bond lengths and bond angles induced by the substituents, termed in-plane nuclear reorganization (IPNR), and not from the deformation themselves. (a) Wertsching, A. K.; Koch, A. S.; DiMagno, S. G. *J. Am. Chem. Soc.* **2001**, *123*, 3932. (b) Ryeng, H.; Ghosh, A. *J. Am. Chem. Soc.* **2002**, *124*, 8099. More recently, Shelnutt and co-workers reexamined the optical shifts experimentally and theoretically and concluded that the red-shifts do indeed result from the nonplanarity of the porphyrin macrocycle rather than from IPNR. (c) Haddad, R. E.; Gazeau, S.; Pecaut, J.; Marchon, J. C.; Medforth, C. J.; Shelnutt, J. A. *J. Am. Chem. Soc.* **2003**, *125*, 1253. It is also unlikely that IPNR can solely account for the other altered properties of nonplanar porphyrins, particularly the often dramatic changes in excited state lifetimes[15,16,36] or the variations in magnetic properties.[5,13,30,37]

(36) (a) Gentemann, S.; Nelson, N. Y.; Jaquinod, L.; Nurco, D. J.; Leung, S. H.; Medforth, C. J.; Smith, K. M.; Fajer, J.; Holten, D. *J. Phys. Chem. B* **1997**, *101*, 1247. (b) Retsek, J. L.; Gentemann, S.; Medforth, C. J.; Smith, K. M.; Chirvony, V. S.; Fajer, J.; Holten, D. *J. Phys. Chem. B* **2000**, *104*, 6690.

(37) Walker, F. A. *Inorg. Chem.* **2003**, *42*, 4526.

(38) Insertion of nonplanar porphyrins into proteins may also prove to be a fruitful avenue of research. Ni tetra(*N*-methylpyridyl)porphyrin has been shown to adopt a distorted conformation in a DNA hexanucleotide duplex. The porphyrin stacks onto the ends of the duplex and also inserts into the minor grooves of the symmetry-related duplex causing "marked distortions from normality" in base pair morphology and providing a viable explanation for porphyrin-induced DNA strand cleavage at deoxyribose residues. Here again, hydrogen bonding is inferred. Bennett, M.; Krah, A.; Wien, F.; Garman, E.; McKenna, R.; Sanderson, M.; Neidle, S. *Proc. Natl. Acad. Sci. U.S.A.* **2000**, *97*, 9476.

(39) For additional examples of conformational variations induced by hydrogen bonding and self-assembly in chlorophyll derivatives see: Barkigia, K. M.; Fajer, J. In *The Photosynthetic Reaction Center*; Deisenhofer, J., Norris, J. R., Eds.; Academic Press: New York, 1993; Vol. II, p 513.